

1 **Fracture properties of GGBFS-blended fly ash**  
2 **geopolymer concrete cured in ambient**  
3 **temperature**

4 Pradip Nath<sup>a,1</sup>, Prabir Kumar Sarker<sup>b</sup>

5 *<sup>a</sup> Department of Civil Engineering, Curtin University, GPO Box U1987, Perth,*  
6 *WA 6845, Australia.*

7 email: [pradip.nath@curtin.edu.au](mailto:pradip.nath@curtin.edu.au)

8 *<sup>b</sup> Department of Civil Engineering, Curtin University, GPO Box U1987, Perth,*  
9 *WA 6845, Australia.*

10 email: [p.sarker@curtin.edu.au](mailto:p.sarker@curtin.edu.au)

11  
12

13 **ABSTRACT**

14 Fracture characteristics are important part of concrete design against brittle failure. Recently, fly  
15 ash geopolymer binder is gaining significant interest as a greener alternative to traditional ordinary  
16 Portland cement (OPC). Hence it is important to understand the failure behaviour of fly ash based  
17 geopolymers for safe design of structures built with such materials. This paper presents the  
18 fracture properties of ambient-cured geopolymer concrete (GPC). Notched beam specimens of  
19 GPC mixtures based mainly on fly ash and a small percentage of ground granulated blast furnace  
20 slag (GGBFS) were subjected to three-point bending test to evaluate fracture behaviour. The effect  
21 of mixture proportions on the fracture properties were compared with control as well as OPC  
22 concrete. The results show that fracture properties are influenced by the mixture compositions.  
23 Presence of additional water affected fracture properties adversely. Fracture energy is generally  
24 governed by tensile strength which correlates with compressive strength. Critical stress intensity  
25 factor varies with the variation of flexural strength. Geopolymer concrete specimens showed  
26 similar load-deflection behaviour as OPC concrete specimens. The ambient cured GPC showed  
27 relatively more ductility than the previously reported heat cured GPC, which is comparable to the  
28 OPC specimens. Fly ash based GPC achieved relatively higher fracture energy and similar values  
29 of  $K_{IC}$  as compared to those of OPC concrete of similar compressive strength. Thus, fly ash based  
30 GPC designed for curing in ambient condition can achieve fracture properties comparable to  
31 normal OPC concrete.

---

<sup>1</sup> Corresponding author: Tel +61 8 9266 7568; Fax +61 8 9266 2681;  
email: [pradip.nath@curtin.edu.au](mailto:pradip.nath@curtin.edu.au)

1 **Keywords:** *Ambient curing, fly ash geopolymer, fracture energy, stress intensity*  
2 *factor.*

## 3 **1 Introduction**

4 Fracture properties such as fracture toughness and fracture energy of a material  
5 are used to describe the formation and progress of cracks in members made of that  
6 material. Furthermore, continuous improvements of binders are improving  
7 concrete behaviour approaching that of a homogeneous material (Juenger et al.  
8 2011). Though concrete is generally referred as a brittle material, it actually  
9 differs from an ideal brittle material in many aspects. In modern fracture  
10 mechanics concrete is considered as a quasi-brittle material exhibiting a post-peak  
11 softening behaviour which lies between a brittle and a ductile material behaviour.  
12 Increased ductility can be provided by increasing the fracture energy by careful  
13 choice of the constituent materials (Bharatkumar et al. 2005; Trussoni et al. 2013)  
14 or by reinforcing the matrix with fibres (Deepa Raj et al. 2013).

15 Fracture characteristics of concrete are influenced by the material properties such  
16 as strength, mixture constituents, and types of aggregate used, and the maturity of  
17 concrete. The size of the specimens is also important factor affecting fracture  
18 properties (Gettu et al.1990). Darwin et al. (2001) found a small variation of  
19 fracture energy of OPC concrete when water-cement ratio varied between 0.25 to  
20 0.45 at any age from 7 days to 180 days. For concretes at least five days old,  
21 fracture energy is independent of compressive strength, w/cm, and age. Fracture  
22 energy of concrete is governed principally by the properties of the coarse  
23 aggregate, with higher strength aggregates (basalt) producing concretes with  
24 higher fracture energies. In contrast, Gettu et al. (1990) found that, as the strength  
25 increases, the fracture energy and the fracture toughness of concrete also increase.

1 In another study on high performance concrete (HPC), the results showed that  
2 there is a reduction in the fracture energy due to addition of fly ash or slag  
3 (Bharatkumar et al. 2005).

4 Geopolymer binder is a relatively new material that requires extensive research  
5 into various properties to ensure its suitability for structural applications. The  
6 binder is produced by chemical reaction of an aluminosilicate material such as fly  
7 ash, blast furnace slag or metakaolin with an alkali (Juenger et al. 2011;  
8 Davidovits 2008). Since geopolymers utilise by-products as the principle source  
9 material, the binders are considered as a low CO<sub>2</sub>-emitting alternative of Portland  
10 cement (Yang et al. 2013). Low-calcium fly ash geopolymer concretes cured in  
11 high temperature have been extensively researched for the last two decades and  
12 are reported to have good mechanical properties (Wallah and Rangan 2003;  
13 Fernandez-Jimenez et al. 2007). The structural properties of heat-cured fly ash  
14 geopolymer concrete were reported to be similar or superior to that of OPC  
15 concrete (Sumajouw et al. 2005; Sarker 2011; Sarker et al. 2013). However,  
16 reports on the structural behavior of ambient-cured geopolymer concrete are  
17 scarce in literature.

18 Sarker et al. (2013) reported fracture properties of heat cured fly ash based  
19 geopolymer concrete and compared with OPC concrete. They found higher peak  
20 load in the geopolymer than the OPC concrete of similar strength grade. The heat-  
21 cured geopolymer concrete specimens were found to be more brittle than the OPC  
22 concrete specimens. Fracture energy was found to be similar in both types of  
23 concrete for similar compressive strengths. The results suggest that the different  
24 fracture behaviour of geopolymer concrete is mainly because of its higher tensile  
25 and bond strengths than OPC concrete of the same compressive strength.

1 Pan et al. (2011) reported the results of experimental research on fracture  
2 properties of heat-cured fly ash based geopolymer concrete and paste with various  
3 mix parameters. The results indicate that the fracture energy and elastic modulus  
4 of geopolymer paste and concrete are lower than those of OPC paste and concrete.  
5 The tensile strength of geopolymer paste and concrete is higher than that of OPC  
6 paste and concrete. The characteristic length of the geopolymer concrete was  
7 approximately three times less than that of ordinary Portland cement (OPC)  
8 concrete. The geopolymer concrete exhibited higher brittleness than its OPC  
9 counterpart.

10 Deepa Raj et al. (2013) worked on the fracture properties of fibre reinforced fly  
11 ash based geopolymer concrete. The study concluded that the load carrying  
12 capacity, deflections and crack mouth opening deflection of geopolymer are more  
13 than those of OPC concrete at ultimate stage. Fracture energy and fracture  
14 toughness are found to be greater than the OPC concrete.

15 These studies reported the properties of fly ash based geopolymers cured in  
16 elevated temperature. High curing temperature and the activation method of the  
17 aluminosilicate source material played the most important roles on the fracture  
18 properties of geopolymers in these studies. However, the fracture behaviour of fly  
19 ash based geopolymer concrete cured in ambient condition has not been studied.  
20 Since the curing method has a significant influence on development of the  
21 hardened properties, it is necessary to study the fracture behaviour of low-calcium  
22 fly ash geopolymer concrete cured at ambient condition. Curing in normal  
23 ambient condition will also help reduce the cost and energy associated with heat  
24 curing. Therefore, this study aimed to investigate the fracture properties of low  
25 calcium fly ash based geopolymer concrete mixtures suitable for curing in

1 ambient condition. Geopolymer concrete mixtures were produced using fly ash as  
2 the principle binder and including a small percentage of GGBFS in order to  
3 improve the setting and hardening properties of the mixtures at the early ages  
4 (Nath and Sarker 2014). Fracture properties such as load-deflection behaviour,  
5 fracture energy and critical stress intensity factor were determined from the test  
6 results. Effects of the mixture variables were evaluated by comparing these  
7 properties for different geopolymer concrete and those of the OPC concrete.

## 8 **2 Experimental program**

### 9 **2.1 Materials**

10 Geopolymer binder was prepared with a Class F fly ash (ASTM C 618), collected  
11 from a West Australian power plant. A commercially available ground granulated  
12 blast furnace slag (GGBFS) was added as a small part of the binder. The chemical  
13 compositions and loss on ignition of fly ash and GGBFS are shown in Table 1.  
14 The alkaline liquid used was a mixture of sodium hydroxide (NaOH) and sodium  
15 silicate ( $\text{Na}_2\text{SiO}_3$ ) solutions. Sodium hydroxide solution of 14 Molar  
16 concentration was prepared by mixing 98-99% pure NaOH pellets with normal  
17 tap water. Sodium silicate solution with  $\text{SiO}_2$  to  $\text{Na}_2\text{O}$  mass ratio of 2.61 ( $\text{SiO}_2 =$   
18  $30.0\%$ ,  $\text{Na}_2\text{O} = 11.5\%$  and water =  $58.5\%$ ) was used. Locally available natural  
19 sand was used as fine aggregate, and coarse aggregates were a combination of  
20 crushed granite with nominal maximum sizes of 7 and 10 mm. The maximum  
21 coarse aggregate size of 10 mm was selected to meet the specification  
22 recommended by RILEM for small size of specimens (RILEM TC 50-FMC 1985).  
23 A superplasticiser (Rheobuild 1000) was used to improve workability. A General

1 purpose ordinary Portland cement (OPC) conforming to Australian standard (AS  
2 3972) was used for the OPC concrete mixture.

## 3 **2.2 Mixture proportions**

4 Concrete mixtures were proportioned to investigate the fracture properties of  
5 ambient cured geopolymer. Mix variables included the amount of GGBFS as a  
6 replacement of fly ash and the amount of alkaline liquid. Five geopolymer  
7 concrete (GPC) and one OPC concrete mixtures were used in the experimental  
8 work. The mixture proportions of concretes are presented in Table 2. Two sets of  
9 mixtures were designed for varying amount of alkaline solution as 40% and 35%  
10 of the total binder. The first set of mixtures were designated as A40 S00, A40 S10  
11 and A40 S15 which contained 40% alkaline liquid and 0%, 10% and 15% GGBFS  
12 respectively. The other set of mixtures contained 35% alkaline liquid and either  
13 0% or 10% GGBFS. The mixtures are designated as A35 S00 and A35 S10  
14 respectively. The ratio of  $\text{Na}_2\text{SiO}_3$  to NaOH solution in the alkaline liquid was  
15 kept constant as 2.5 for all the geopolymer mixtures.

16 The slump test was conducted to measure workability of the mixtures. Mixtures  
17 having 40% alkaline liquid achieved more than 200 mm slump after mixing which  
18 is similar to that obtained in our previous study (Nath and Sarker 2014). Mixtures  
19 having 35% alkaline liquid generally show lower workability. Hence, additional  
20 water and superplasticiser were used in the mixtures having 35% alkaline liquid to  
21 achieve similar slump values of mixtures having 40% alkaline liquid.

## 22 **2.3 Casting and curing of the test specimens**

23 The beam specimen for fracture test was 600 mm in length and  $100 \times 100$  mm in  
24 cross section. The geometric dimensions of all the test specimens were kept

1 constant. A 25 mm deep notch was cast at the mid-section of the beam. Different  
2 notch depths were used for fracture tests by different researchers (Gettu et al.  
3 1990; Sarker et al. 2013; Pan et al. 2011) in literature. However, previous studies  
4 conducted with different notch-depth ratio revealed comparable results as long as  
5 the specimen size remained constant. In this study a notch-depth ratio of 0.25 was  
6 used after some trials with 0.25 and 0.50. The smaller ratio of 0.25 was selected to  
7 reduce the chance of accidental cracking during de-moulding and handling of the  
8 test specimens. It also ensured the ligament area sizable enough to observe the  
9 crack propagation in the concrete. The mould was designed to facilitate carving  
10 the notch while casting the specimen. Companion cylinder and prism specimens  
11 were cast for compressive strength, modulus of elasticity and flexural strength  
12 tests.

13 The geopolymer mixtures were mixed in a laboratory pan-mixer. The premixed  
14 alkaline liquid was added gradually to the dry mixture of aggregates and binders  
15 (fly ash and GGBFS). The mixing was then continued for 4 to 6 minutes until a  
16 consistent mixture was obtained. The fresh concrete mixture was cast in the  
17 moulds in two layers. Each layer was compacted using a vibrating table. The  
18 moulds with finished concrete specimens were moved to the curing room (18-23  
19 °C and  $70 \pm 10\%$  RH) immediately after casting. After 24 hours, the specimens  
20 were de-moulded and stored in the same condition (18-23°C and  $70 \pm 10\%$  RH)  
21 until tested. Note that the specimens were not subjected to heat curing. The GPC  
22 specimens without GGBFS (A40 S00 and A35 S00) were de-moulded three days  
23 after casting, because of the long setting time required for these mixtures.

24 To compare with the properties of GPC mixtures, an OPC concrete mixture was  
25 designed in accordance with the ACI guideline (ACI 2011.1-91). The OPC

1 concrete specimens were immersed in water after de-moulding on the day after  
2 casting. The specimens were removed from water after 28 days and stored in the  
3 same condition as the geopolymer samples until tested.

#### 4 **2.4 Test methods**

5 Three-point bending test was conducted to determine fracture properties of the  
6 concrete specimens following the RILEM guidelines (RILEM TC 50 – FMC  
7 1985). The beam was simply supported over a span of 500 mm with the notched  
8 face down and a single point load was applied at the centre of the beam (Figure  
9 1). To reduce the effect of friction between the loading platen and the specimen,  
10 ball bearing support apparatus were used in accordance with the ASTM  
11 (C78/C78M-10e) standard. The test was conducted using a closed-loop universal  
12 testing machine (Instron Servo Control machine). The specimen was loaded to  
13 induce a vertical mid-section deflection at a rate of 0.5 mm/min. This loading rate  
14 was selected after several trial tests to ensure the maximum load is reached within  
15 30–60 seconds as recommended in the RILEM guidelines. The load and vertical  
16 deflection data were recorded by an automatic data acquisition system at rate of  
17 100 readings per second. The accuracies of the load and deflection data were to  
18 0.001 kN and 0.001 mm respectively. Load was applied until complete failure of  
19 the specimen. Three identical specimens were tested for each of the mixtures at  
20 both 28 and 90 days. Since the strength of ambient-cured geopolymers continue to  
21 develop beyond 28 days, the test was extended to 90 days in order to understand  
22 the influence of age on the fracture properties.

23 Compressive strength test was conducted at the age of 28 and 90 days. Cylinder  
24 specimens (100 mm diameter and 200 mm height) were tested at a loading rate of  
25 0.33 MPa/s. Testing for flexural strength was conducted following the Australian



1 Standard (AS 1012.11-2000). The test involves beam specimens of dimensions  
2 100 mm × 100 mm × 400 mm loaded in pure bending to fail due to flexural stress.  
3 Modulus of elasticity of concrete samples was determined according to the ASTM  
4 standard (ASTM C 469/C 469M - 10).

## 5 **2.5 Evaluation of fracture parameters**

6 After the test, the load-deflection graph was plotted with the recorded data. The  
7 fracture energy ( $G_F$ ) was calculated by the work of fracture method using  
8 Equation 1 given in the RILEM guidelines (RILEM TC 50-FMC 1985). It is the  
9 summation of the work done by the external load calculated by the area under the  
10 load-deflection curve, ( $W_o$ ) and work done by self-weight of the beam.

$$11 \quad G_F = \frac{W_o + mg \delta_o}{A_{lig}} \quad (1)$$

12 where  $W_o$  = area under the load-deflection curve (N-m),  $m$  = mass of the beam  
13 between the support (kg),  $g$  = acceleration due to gravity (9.81 m/s<sup>2</sup>),  $\delta_o$  = the  
14 deflection at the final failure of the beam (m) and  $A_{lig}$  = area of the ligament (m<sup>2</sup>).

15 The experimental values of fracture energy were compared with some established  
16 model equations proposed in the literature for OPC concrete. The CEB-FIP  
17 committee recommended a prediction formula as given by Eq. 2 (Bazant and Becq-  
18 Giraudon 2002).

$$19 \quad G_F = (0.0469s^2 - 0.5s + 26) \left( \frac{f'_c}{10} \right)^{0.7} \quad (2)$$

20 where,  $s$  = maximum aggregate size (mm),  $f'_c$  = compressive strength of concrete  
21 (MPa)

1 Another equation (Eq. 3) was proposed by Bazant and Becq-Giraduon (2002)  
 2 following a statistical analysis of 238 test data on fracture energy of OPC concrete  
 3 of strength and age varying in a wide range. The coefficient of variation of the test  
 4 to prediction ratios of the results by this equation was found to be 29.9%. The  
 5 equation takes into account the compressive strength, maximum aggregate size  
 6 and the water to cement ratio of the concrete. Since geopolymer concrete is  
 7 different from the usual mixture of OPC concrete, the term liquid to binder ratio  
 8 of geopolymer mixture, as shown in Table 2, was used as equivalent to the water  
 9 to cement ratio of OPC concrete. The liquid content was calculated by adding the  
 10 amount of NaOH solution, Na<sub>2</sub>SiO<sub>3</sub> solution and any extra water. Total binder  
 11 content includes the binders such as fly ash and GGBFS.

$$12 \quad G_F = 2.5 \alpha_o \left( \frac{f'_c}{0.051} \right)^{0.46} \left( 1 + \frac{s}{11.27} \right)^{0.22} \left( \frac{w}{c} \right)^{-0.30} \quad (3)$$

13 where,  $\alpha_o$  is aggregates shape factor (1 for round aggregates, 1.44 for angular or  
 14 crushed aggregates), and  $w/c$  is the water to cement ratio of the OPC concrete.

15 The critical stress intensity factor ( $K_{IC}$ ) was calculated using Equation 4 (Peterson  
 16 1980). It is also known as fracture toughness and relates to the peak load and the  
 17 geometric dimensions of the beam.

$$18 \quad K_{IC} = \frac{3P_{max}l}{2bd^2} \sqrt{a_o} (1.93 - 3.07A + 14.53A^2 - 25.11A^3 + 25.8A^4) \quad (4)$$

19 where,  $P_{max}$  = the peak load,  $l$  = the span of beam,  $b$  = the width of beam,  $d$  = the  
 20 depth of beam,  $a_o$  = the depth of the notch and  $A = a_o/d$ .

## 1   **3   Results and discussion**

### 2   **3.1   Mechanical properties**

#### 3   **3.1.1   Compressive strength**

4   Mechanical properties of all the mixtures were determined at the same time when  
5   the three-point bending tests were conducted. Results of compressive strength,  
6   flexural strength and modulus of elasticity are given in Table 3. The compressive  
7   strength and modulus of elasticity are also plotted in Figure 2. The 28-day  
8   compressive strength of the geopolymer concretes of this study varied from 25  
9   MPa to 46 MPa and increased up to 53 MPa at 90 days. It is clear from the results  
10   that the compressive strength enhanced significantly with the increase of GGBFS  
11   content in the mixtures designed with 40% alkaline liquid (Figure 2). The  
12   improvement of strength due to inclusion of GGBFS followed the same trend as  
13   reported in previous study (Nath and Sarker 2014). The increase of strength was  
14   also observed when the alkaline liquid was reduced to 35% and no extra water  
15   was added (mixture A35 S00). However, mixture A35 S10 showed lower strength  
16   than that having 40% alkaline liquid and same additive content of 10% GGBFS  
17   (A40 S10). This reduction in strength is caused by the addition of extra water  
18   along with superplasticiser in the mixture A35 S10 (Table 2). The additional  
19   water reduced the concentration of alkaline liquid which eventually decreased  
20   strength. The geopolymer mixtures containing 35% alkaline liquid with or without  
21   10% GGBFS resulted in similar compressive strengths. This result implies that  
22   the inclusion of a small amount of GGBFS such as 10% can balance the negative  
23   effect of additional water on the strength development of geopolymer concrete.

### 1 **3.1.2 Flexural strength**

2 It can be seen from Table 3 that flexural strength of geopolymer concrete cured in  
3 ambient temperature increased with age for all the mixtures. This is similar to the  
4 development of compressive strength with age, as observed in Figure 2. Also,  
5 flexural strength increased with the inclusion of GGBFS content up to 10%. A  
6 slight decline in the flexural strength was observed for increasing the GGBFS  
7 content to 15%. From Table 3 it can be seen that, mixture A35 S10, having  
8 additives and extra water in the mixtures, achieved about 30% less flexural  
9 strength than that of control geopolymer A35 S00 which had no water added.  
10 While mixtures having 35% alkaline liquid only with no extra water achieved  
11 higher compressive and flexural strength, addition of water with 35% alkaline  
12 activator in concretes having GGBFS have decreased flexural strength. This  
13 indicates that the presence of extra water adversely affected flexural tensile  
14 strength of ambient cured geopolymer concrete.

15 When compared with OPC concrete, geopolymer concrete of similar strength  
16 (A40 S10) exhibited higher flexural tensile strength than the OPC concrete (Table  
17 3). The result is consistent with that reported for both heat cured (Hardjito 2005;  
18 Rangan 2007) and ambient cured geopolymer concretes (Deb et al. 2014).

### 19 **3.1.3 Modulus of elasticity**

20 Generally, the value of modulus of elasticity varied with the compressive strength  
21 and no significant difference is observed due to variation of the mixture  
22 proportions. Similar trends were observed at the ages of 28 days and 90 days, as  
23 shown in Figure 2. Geopolymer concretes cured in elevated temperature generally  
24 reported to have low modulus of elasticity as compared to that of OPC concrete of  
25 the same compressive strength (Fernandez-Jimenez et al. 2006; Sofi et al. 2007).

1 The ambient cured geopolymer concretes of this study also showed similar trends.  
2 It can be seen from Table 3 that the modulus of elasticity of geopolymer concretes  
3 are relatively less than the OPC concrete of similar compressive strength. For a 40  
4 MPa concrete, while OPC mixture had modulus of elasticity of 30.6 GPa, similar  
5 grade geopolymer concrete (A40 S10) achieved a modulus of elasticity of 22.6  
6 GPa at 28 days. This is about 24% less than OPC concrete at 28 days and the  
7 difference increased to 29% after 90 days. In a previous study, heat cured  
8 geopolymer concrete showed about 22% less modulus of elasticity than OPC  
9 concrete (Pan et al. 2011).

## 10 **3.2 Fracture properties**

### 11 **3.2.1 Load-deflection behaviour**

12 Typical load deflection patterns of fly ash geopolymers containing GGBFS along  
13 with 40% alkaline solution, and the OPC concrete are presented in Figure 3. The  
14 initial non-linearity of the load–deflection curves were corrected to eliminate  
15 distortions caused by the deformation of the specimen at the supports and  
16 adjustments at contact planes (Sarker et al. 2013; RILEM TC 50-FMC 1985). Figure  
17 3 shows the load deflection diagrams of different specimens at 28 days and 90  
18 days. As usual, the curve showed a linear upward slope until the load reached  
19 cracking limit of the material. It can be seen from the graphs that the slope of the  
20 pre-peak curve generally increased for the specimens having higher strength than  
21 control concrete (A40 S00). After reaching peak load, the crack initiates which  
22 results in a downward post peak curve. The slope of post-peak part of the curve  
23 reflects the property of the cracked specimen until breaking. The curvature of post  
24 peak curve varied depending on the ductility of the material. The slope gradually

1 decreased with the increase of the compressive strength of the geopolymer  
2 concretes. This indicates reduced ductility of the specimens with increasing  
3 compressive strength. The control specimen of A40 S00, which had lowest  
4 strength, showed greater stretch of the post peak curve before complete failure.  
5 The load-deflection curves of geopolymer concretes are of similar shape as that of  
6 OPC concrete. However, the pre-peak slopes of the curve appeared slightly  
7 steeper in case of geopolymer specimens. This implies that OPC concrete of  
8 similar grade tend to deflect more than geopolymer concretes before initiating the  
9 crack. The post peak behaviour is almost similar for OPC and ambient cured  
10 geopolymer concretes as indicated by the similar post-peak slopes. This is  
11 different from that observed in the study of heat cured fly ash based geopolymer  
12 concrete (Sarker et al. 2013). It is reported that, the post-peak load usually  
13 dropped faster in the heat cured specimens than in the OPC concrete specimens  
14 and showed a steeper slope of the post-peak curve. However, in this study of  
15 ambient cured GPC, the post peak slope of load deflection diagram for both GPC  
16 and OPC concrete gradually decreased rather than dropping sharply. Geopolymer  
17 specimens showed relatively slightly greater stretch of deflection before ultimate  
18 failure than OPC concrete at both 28 and 90 days. Hence it can be stated that  
19 ambient cured GPC showed more ductile behaviour than heat cured GPC which is  
20 comparable to that of OPC concrete.

### 21 **3.2.2 Peak load**

22 Peak load as a fracture property indicates the maximum load that is required to the  
23 separate the surfaces involving in the crack which takes place across an extended  
24 crack tip, or cohesive zone (Dugdale 1960). Peak loads of all the specimens are  
25 given in Table 4. The average peak loads of ambient cured geopolymer concrete

1 varied in the range of 2.7 to 4.5 kN at 28 days and 3.2 to 5.2 kN at 90 days. Figure  
2 4 shows the variations of average peak load and the flexural strength of the  
3 concretes. At both the ages of 28 and 90 days, the peak load varied in the same  
4 way as flexural strength of the concrete. Among the geopolymer concretes,  
5 mixture A35 S00 showed the maximum peak load as well as flexural strength.  
6 The mixture composition mainly influenced the flexural strength which led to the  
7 variation of peak load value in three-point bending tests. The OPC concrete has  
8 less flexural strength than the geopolymer concrete of equal grade (A40 S10);  
9 however, OPC concrete showed similar peak load as compared to similar grade  
10 geopolymer concrete. Heat cured fly ash based geopolymer generally showed  
11 higher peak load as compared to OPC concrete (Sarker et al. 2013).

### 12 **3.2.3 Fracture energy**

13 Fracture energy ( $G_F$ ) was calculated by the work of fracture method (Eq. 1).  
14 Results of three-point bending tests are presented in Table 4. Fracture energy of  
15 the geopolymer concretes varied in the range of 150 - 232.8 N/m at 28 days and  
16 172.4 - 250.4 N/m at 90 days. The mean fracture energy values of the geopolymer  
17 and OPC concrete mixtures are compared in Figure 5. It can be seen that the  
18 mixture proportions of geopolymer concrete have influenced the fracture energy.  
19 Generally, the fracture energy of geopolymer concretes tends to increase with the  
20 increase of GGBFS up to 10% in the mixture. Regardless of alkaline solution  
21 content, mixtures having GGBFS as partial replacement of fly ash showed higher  
22 fracture energy as compared to the control geopolymers (A40 S00 and A35 S00).  
23 Comparing between the controls, mixture A35 S00, which was mixed with 35%  
24 alkaline liquid and superplasticiser, showed relatively less fracture energy albeit  
25 achieving higher compressive strength than mixture A40 S00. When water and

1 superplasticiser were added in addition to 35% alkaline solution in the mixture,  
2 these affected the fracture characteristics. For instance, mixture A40 S10 achieved  
3 higher compressive strength and fracture energy (223.1 N/m at 28 day) than those  
4 of mixture A35 S10 (197 N/m at 28 days).

5 Fly ash based geopolymer concrete of similar compressive strength achieved  
6 relatively higher fracture energy than OPC concrete. For instance, mixture A40  
7 S10 achieved 26% more fracture energy at 28 days and mixture A40 S15 achieved  
8 37% more fracture energy at 90 days as compared to OPC concrete. Sarker et al  
9 (2013) found that the fracture energy of heat cured GPC tends to increase with  
10 compressive strength at a higher rate than OPC concrete. The mean 28-day and  
11 90-day fracture energy values of this study and previous results on heat cured  
12 GPC (Sarker et al. 2013) are plotted against compressive strength in Figure 6. It is  
13 apparent that fracture energy of the ambient cured GPC increase with the increase  
14 of compressive strength regardless of the age. The rate of increase is, however,  
15 similar to the OPC concrete. It can be noted from Figure 6 that the fracture energy  
16 values of ambient cured GPC were higher than those of the heat cured GPC. This  
17 is probably due to increased brittleness of heat cured specimens that caused abrupt  
18 failure of the concrete after reaching the peak load. As observed in load-deflection  
19 curves, the ambient cured specimens of this study showed a gradual post peak  
20 progression (Figure 3) rather than abrupt failure and resulted in larger work done  
21 (fracture energy).

22 Figure 6 also compares the fracture energy values obtained from experiment with  
23 those calculated using the prediction equations proposed by CEB-FIP (Eq. 2) and  
24 Bazant & Becq-Giraduon (2002) (Eq. 3). The experimental values were found to  
25 be significantly higher than those predicted using the CEB-FIP equation, whereas



1 the equation of Bazant & Becq-Giraduon predicted values relatively closer to the  
2 experiment. However, this equation, which was originally developed from the  
3 results of OPC concretes, calculated lower values of fracture energy for  
4 geopolymer concrete. As observed in this study fly ash based geopolymer  
5 concretes generally show higher fracture energy than that of OPC concrete. Hence  
6 the equation of Bazant & Becq-Giraduon (2002) can be used conservatively for  
7 preliminary estimate of fracture energy of fly ash based GPC cured in ambient  
8 condition.

#### 9 **3.2.4 Critical stress intensity factor**

10 Figure 7 shows the variation of the critical stress intensity factor ( $K_{IC}$ ) with  
11 respect to compressive strength of the studied mixtures of geopolymer and OPC  
12 concrete at 28 and 90 days of age. The value of  $K_{IC}$  showed a gradual increasing  
13 trend with the increase of strength. The geopolymer mixtures followed similar  
14 values of  $K_{IC}$  as OPC concrete of similar compressive strength. This is different  
15 from that reported for heat cured geopolymer which showed higher  $K_{IC}$  values as  
16 compared to OPC concrete (Sarker et al. 2013). Compressive strength of the  
17 mixtures played a significant role on the fracture parameters. However, some of  
18 the mixtures, especially those having 35% alkaline liquid, showed different trend  
19 which is more related to flexural tensile strength. Hence the values of  $K_{IC}$  of  
20 different mixtures have been compared to flexural strength (modulus of rupture)  
21 in Figure 8. It is evident that the values of  $K_{IC}$  followed the same trend of flexural  
22 tensile strength development for all of the mixtures. The critical stress intensity at  
23 the crack tip is governed by the peak load of concrete, which is also related to  
24 tensile strength.

1 From Table 4 it can be seen that, most of the geopolymer mixtures followed the  
2 trend of increasing fracture energy with the increasing value of  $K_{IC}$ . However,  
3 mixtures A35 S00, which has only fly ash as the binder, 35% alkaline solution and  
4 no extra water in the mix, showed comparatively high  $K_{IC}$  but less fracture energy  
5 at both ages of 28 and 90 days as compared to other control concrete A40 S00 and  
6 concretes having GGBFS with fly ash. This is due to its (A35 S00) high flexural  
7 tensile strength and increased brittleness. This suggests that the geopolymer  
8 concretes which were mixed with 35% alkaline liquid only tend to produce  
9 geopolymer gel with relatively low fracture resisting capacity, i.e. low fracture  
10 energy but high  $K_{IC}$ .

## 11 **4 Conclusions**

12 This study investigated fracture behaviour of fly ash based geopolymer concrete  
13 cured in ambient condition. Geopolymer concretes were prepared with mainly fly  
14 ash as the binder and GGBFS as an additive. Fracture properties were investigated  
15 by three-point bending test of notched beam specimens. The following  
16 conclusions are drawn from the results of the study:

- 17 • Inclusion of GGBFS in fly ash geopolymer enhanced compressive strength.  
18 Flexural strength increased when GGBFS was added up to 10% of total binder.  
19 The flexural strength of geopolymer concretes was higher than the OPC  
20 concrete of similar compressive strength. When water was added with 35%  
21 alkaline solution to facilitate workability, it caused an adverse effect on the  
22 compressive and flexural strengths.
- 23 • Modulus of elasticity of geopolymer concrete varied likewise as compressive  
24 strength. No adverse effect on the modulus of elasticity was seen for the

1 presence of GGBFS in addition to fly ash in the mixture. Similar to heat cured  
2 geopolymer concrete, the modulus of elasticity of ambient cured geopolymer  
3 concrete was less than that of OPC concrete of the same compressive strength.

- 4 • The ambient cured GPC specimens showed similar load-deflection behaviour  
5 to that of OPC concrete. The ambient cured GPC showed relatively more  
6 ductility than the reported heat cured specimens, which is comparable to the  
7 OPC specimens. The peak load initiating crack varied with the flexural strength  
8 of concrete.
- 9 • Generally, the fracture energy and critical stress intensity factor increased with  
10 the increase of compressive strength regardless of age. The values of  $K_{IC}$   
11 showed the same trend of flexural tensile strength. The fracture energy of  
12 concrete having GGBFS as an additive to fly ash was higher than that having  
13 fly ash only. Fly ash based GPC achieved relatively higher fracture energy and  
14 similar values of  $K_{IC}$  as compared to those of OPC concrete of similar  
15 compressive strength. Ambient cured GPC resulted in higher fracture energy  
16 values than that of the heat cured GPC.
- 17 • Geopolymer concretes which were mixed with 35% alkaline solution only  
18 tend to produce geopolymer gel with relatively low fracture resisting capacity,  
19 i.e. low fracture energy but high  $K_{IC}$ . When water was added in the GGBFS-  
20 blended mixture with 35% alkaline solution, similar compressive strength,  
21 higher fracture energy as compared to control mixture.

22 Finally, the mixture proportion of geopolymer and curing condition has  
23 significant influence on the fracture properties. Fly ash based geopolymer  
24 concrete designed for curing in ambient condition can achieve fracture properties  
25 comparable to normal OPC concrete.

## 1    **5    Acknowledgement**

2    The authors wish to gratefully acknowledge the support of Coogee Chemicals regarding supply of  
3    the chemicals. The authors also acknowledge the use of equipment, scientific and technical  
4    assistance of the Curtin University, Australia.

## 5    **6    Compliance with Ethical Standards**

6    **Funding:** This study was not funded.

7    **Conflict of Interest:** The authors declare that they have no conflict of interest.

8

## 9    **7    References**

- 10   AS 3972 (1997) Portland and blended cements. Standards Australia; February.
- 11   ACI 211.1-91 (1991) Standard Practice for Selecting Proportions for Normal Heavyweight, and  
12       Mass Concrete. ACI Committee 211, American Concrete Institute, Farmington Hills, MI  
13       48331 U.S.A.
- 14   AS 1012.11-2000 (2000) Methods of testing concrete – Method 11: Determination of the modulus  
15       of rupture. Standards Australia.
- 16   ASTM C78/C78M-10e (2010) Standard Test Method for Flexural Strength of Concrete (Using  
17       Simple Beam with Third-Point Loading. ASTM Standard. ASTM International, West  
18       Conshohocken, PA.
- 19   ASTM C469/C469M – 10 (2010). Standard Test Method for Static Modulus of Elasticity and  
20       Poisson’s Ratio of Concrete in Compression. ASTM Standards. ASTM International, West  
21       Conshohocken, PA.
- 22   ASTM C 618 (2008) Standard specification for coal fly ash and raw or calcined natural pozzolan  
23       for use in concrete. ASTM International, West Conshohocken, PA.
- 24   Bazant ZP, Becq-Giraudon E (2002) Statistical prediction of fracture parameters of concrete and  
25       implications for choice of testing standard. *Cem Conc Res* 32(4):529-556. doi:10.1016/s0008-  
26       8846(01)00723-2
- 27   Bharatkumar BH, Raghuprasad BK, Ramachandramurthy DS, Narayanan R, Gopalakrishnan S  
28       (2005) Effect of fly ash and slag on the fracture characteristics of high performance concrete.  
29       *Mater Struct* 38(1):63-72. doi:10.1007/bf02480576
- 30   Deb PS, Nath P, Sarker PK (2014) The effects of ground granulated blast-furnace slag blending  
31       with fly ash and activator content on the workability and strength properties of geopolymer  
32       concrete cured at ambient temperature. *Mater Des* 62:32-39. doi:10.1016/j.matdes.2014.05.001
- 33   Darwin D, Barham S, Kozul R, Luan S (2001) Fracture Energy of High-Strength Concrete. *ACI*  
34       *Mater J* 98(5):411-417. doi:10.14359/10731

- 1 Davidovits J (2008) *Geopolymer Chemistry and Application*. 2nd ed. Saint-Quentin, France:  
2 Institut Géopolymère.
- 3 Deepa Raj S, Abraham R, Ganesan N, Sasi D (2013) Fracture Properties of Fibre Reinforced  
4 Geopolymer Concrete. *Inter J Sci Eng Res* 4(5):75-80.
- 5 Dugdale, D. S. (1960). Yielding of steel sheets containing slits. *Journal of the Mechanics and*  
6 *Physics of Solids*, 8(2), 100-104.
- 7 Fernandez-Jimenez A, Garcia-Lodeiro I, Palomo A (2007) Durability of alkali-activated fly ash  
8 cementitious materials. *J Mater Sci* 42(9):3055–65.
- 9 Fernandez-Jimenez AM, Palomo A, Lopez Hombrados C (2006) Engineering Properties of Alkali-  
10 activated Fly Ash Concrete. *ACI Mater J* 103(2):106–112. doi:10.14359/15261
- 11 Gettu R, Bazant ZP, Karr KE (1990) Fracture Properties and Brittleness of High- Strength  
12 Concrete. *Mater J* 87(6):608-618. doi:10.14359/2513
- 13 Hardjito D (2005) Studies of fly ash-based geopolymer concrete. Doctoral Dissertation. Curtin  
14 University, Perth, Australia.
- 15 Hillerborg AM (1985) The Theoretical Basis of a Method to Determine the Fracture Energy of  
16 Concrete. RILEM Technical Committees, pp. 291-296.
- 17 Juenger MCG, Winnefeld F, Provis J, Ideker J (2011) Advances in alternative cementitious  
18 binders. *Cem Conc Res* 41(12):1232-1243. doi:10.1016/j.cemconres.2010.11.012
- 19 Nath P, Sarker PK (2014) Effect of GGBFS on setting, workability and early strength properties of  
20 fly ash geopolymer concrete cured in ambient condition. *Const Build Mater* 66:163–171. DOI:  
21 10.1016/j.conbuildmat.2014.05.080
- 22 Pan Z, Sanjayan JG Rangan BV (2011) Fracture properties of geopolymer paste and concrete. *Mag*  
23 *Conc Res* 63(10):763-771.
- 24 Peterson PE (1980) Fracture energy of concrete: Method of determination. *Cem Conc Res*  
25 10(1):79-89. doi:10.1016/0008-8846(80)90054-x
- 26 Rangan BV (2007) Low-calcium fly ash-based geopolymer concrete. In Nawy EG (ed.) *Concrete*  
27 *Construction Engineering Handbook*, 2nd ed. New York: CRC Press.
- 28 RILEM TC 50-FMC (1985) Draft recommendation: Determination of the fracture energy of  
29 mortar and concrete by means of three-point bend tests on notched beams. *Mater and Struct*,  
30 18(6), 285-290, doi:10.1007/bf0249875718.
- 31 Sarker PK (2011) Bond strength of reinforcing steel embedded in geopolymer concrete. *Mater*  
32 *Struct* 44(5):1021–30.
- 33 Sarker PK, Haque R, Ramgolam KV. (2013) Fracture behaviour of heat cured fly ash based  
34 geopolymer concrete. *Mater Des* 44:580–86.
- 35 Sofi M, van Deventer JSJ, Mendis PA, Lukey GC (2007) Engineering properties of inorganic  
36 polymer concretes (IPCs). *Cem Conc Res* 37(2):251-257.  
37 doi:10.1016/j.cemconres.2006.10.008
- 38 Sumajouw DMJ, Hadrijito D, Wallah SE, Rangan BV (2005) Flexural behaviour of reinforced fly  
39 ash-based geopolymer concrete beams. In: Proc. of CONCRETE 05 Conference, Melbourne,  
40 Concrete Institute of Australia; October.

- 1 Trussoni M, Hays CD, Zollo RF (2013) Fracture Properties of Concrete Containing Expanded
- 2 Polystyrene Aggregate Replacement. *ACI Mater J* 110(5). doi:10.14359/51685906
- 3 Wallah SE, Rangan BV (2006) Low-calcium fly ash-based geopolymer concrete: long-term
- 4 properties. Research Report GC 2, Perth, Australia: Faculty of Engineering, Curtin University
- 5 of Technology.
- 6 Yang KH, Song JK, Song KI (2013) Assessment of CO<sub>2</sub> reduction of alkali-activated concrete. *J*
- 7 *Clean Prod* 39:265-72.
- 8

**Table 1:** Chemical composition of fly ash and GGBFS.

|                    | SiO <sub>2</sub> | Al <sub>2</sub> O <sub>3</sub> | Fe <sub>2</sub> O <sub>3</sub> | CaO   | MgO | Na <sub>2</sub> O | K <sub>2</sub> O | SO <sub>3</sub> | P <sub>2</sub> O <sub>5</sub> | TiO <sub>2</sub> | LOI* |
|--------------------|------------------|--------------------------------|--------------------------------|-------|-----|-------------------|------------------|-----------------|-------------------------------|------------------|------|
| <b>Fly ash (%)</b> | 53.71            | 27.2                           | 11.7                           | 1.9   | -   | 0.36              | 0.54             | 0.3             | 0.71                          | 1.62             | 0.68 |
| <b>GGBFS (%)</b>   | 29.96            | 12.25                          | 0.52                           | 45.45 | -   | 0.31              | 0.38             | 3.62            | 0.04                          | 0.46             | 2.39 |

\* Loss on ignition

**Table 2:** Mixture proportions of GPC and OPC concrete (kg/m<sup>3</sup>)

| Mix ID  | Coarse aggregate |       |       | Binders |       |       | Alkaline solutions               |      |       | Super-plasticizer | Water/solid (w/s) |
|---------|------------------|-------|-------|---------|-------|-------|----------------------------------|------|-------|-------------------|-------------------|
|         | 10 mm            | 7 mm  | Sand  | Fly ash | GGBFS | OPC   | Na <sub>2</sub> SiO <sub>3</sub> | NaOH | Water |                   |                   |
| A40 S00 | 651              | 558   | 651   | 400     | 0     | -     | 114.3                            | 45.7 | 0     | 0                 | 0.202             |
| A40 S10 | 651              | 558   | 651   | 360     | 40    | -     | 114.3                            | 45.7 | 0     | 0                 | 0.202             |
| A40 S15 | 651              | 558   | 651   | 340     | 60    | -     | 114.3                            | 45.7 | 0     | 0                 | 0.202             |
| A35 S00 | 655.9            | 562.2 | 655.9 | 400     | 0     | -     | 100                              | 40   | 0     | 6                 | 0.180             |
| A35 S10 | 655.9            | 562.2 | 655.9 | 360     | 40    | -     | 100                              | 40   | 6     | 6                 | 0.193             |
| OPC     | 430.4            | 368.8 | 921.4 | -       | -     | 387.9 | -                                | -    | 213.4 | 0                 | 0.55*             |

\* water/cement (w/c) ratio for OPC concrete.

**Table 3:** Strength and modulus of elasticity results

| Mixture | Compressive strength, $f_{cm}$ (MPa) |        | Flexural Strength $f_{ct,f}$ (MPa) |        | Modulus of Elasticity, E (GPa) |        |
|---------|--------------------------------------|--------|------------------------------------|--------|--------------------------------|--------|
|         | 28 day                               | 90 day | 28 day                             | 90 day | 28 day                         | 90 day |
| A40 S00 | 25.6                                 | 33.4   | 4.89                               | 5.91   | 17.4                           | 20.0   |
| A40 S10 | 38.3                                 | 45.5   | 5.79                               | 6.47   | 22.6                           | 23.8   |
| A40 S15 | 46.6                                 | 53.3   | 5.26                               | 6.12   | 24.6                           | 25.2   |
| A35 S00 | 32.5                                 | 41.1   | 6.13                               | 7.68   | 19.8                           | 22.8   |
| A35 S10 | 33.3                                 | 43.0   | 4.27                               | 5.52   | 19.2                           | 22.2   |
| OPC     | 41.6                                 | 50.6   | 3.68                               | 4.97   | 30.6                           | 33.4   |

**Table 4:** Fracture properties of ambient cured fly ash based geopolymers and OPC concretes at 28 and 90 days.

| Mix ID  | 28 days          |                |             |                  |                                   |                                        | 90 days          |                |             |                  |                                   |                                        |
|---------|------------------|----------------|-------------|------------------|-----------------------------------|----------------------------------------|------------------|----------------|-------------|------------------|-----------------------------------|----------------------------------------|
|         | Mean $f_c$ (MPa) | $P_{max}$ (kN) | $G_F$ (N/m) | Mean $G_F$ (N/m) | $K_{IC}$ (MPa-mm <sup>1/2</sup> ) | Mean $K_{IC}$ (MPa-mm <sup>1/2</sup> ) | Mean $f_c$ (MPa) | $P_{max}$ (kN) | $G_F$ (N/m) | Mean $G_F$ (N/m) | $K_{IC}$ (MPa-mm <sup>1/2</sup> ) | Mean $K_{IC}$ (MPa-mm <sup>1/2</sup> ) |
| A40 S00 | 25.6             | 2.73           | 157.7       | 156.3            | 15.9                              | 15.7                                   | 33.4             | 3.27           | 227.1       | 206.4            | 16.6                              | 19.4                                   |
|         |                  | 2.74           | 154.9       |                  | 15.5                              |                                        |                  | 3.12           | 184.7       |                  | 19.9                              |                                        |
|         |                  | -              | -           |                  | -                                 |                                        |                  | 3.42           | 207.3       |                  | 21.6                              |                                        |
| A40 S10 | 38.3             | 3.72           | 191.6       | 223.1            | 22.5                              | 23.1                                   | 45.5             | 3.69           | 214.0       | 234.6            | 22.0                              | 21.9                                   |
|         |                  | 3.61           | 216.9       |                  | 22.0                              |                                        |                  | 3.60           | 216.5       |                  | 20.9                              |                                        |
|         |                  | 4.02           | 261.0       |                  | 24.7                              |                                        |                  | 3.76           | 273.2       |                  | 22.7                              |                                        |
| A40 S15 | 46.6             | 3.61           | 231.0       | 201.3            | 22.8                              | 21.7                                   | 53.3             | 3.67           | 201.8       | 250.5            | 23.1                              | 25.6                                   |
|         |                  | 3.60           | 200.6       |                  | 22.4                              |                                        |                  | 4.24           | 305.8       |                  | 27.3                              |                                        |
|         |                  | 3.55           | 172.2       |                  | 19.8                              |                                        |                  | 4.37           | 244.0       |                  | 26.4                              |                                        |
| A35 S00 | 32.5             | 4.89           | 168.1       | 150.0            | 28.8                              | 26.6                                   | 41.1             | 5.90           | 179.4       | 172.4            | 30.8                              | 29.5                                   |
|         |                  | 4.53           | 145.9       |                  | 26.7                              |                                        |                  | 5.05           | 185.0       |                  | 25.6                              |                                        |
|         |                  | 4.09           | 136.0       |                  | 24.3                              |                                        |                  | 4.88           | 153.0       |                  | 29.0                              |                                        |
| A35 S10 | 33.3             | 3.33           | 197.7       | 197.0            | 20.6                              | 20.3                                   | 43.0             | 4.12           | 207.5       | 175.4            | 24.0                              | 21.2                                   |
|         |                  | -              | -           |                  | -                                 |                                        |                  | 3.07           | 143.3       |                  | 18.3                              |                                        |
|         |                  | 3.29           | 196.3       |                  | 20.1                              |                                        |                  | -              | -           |                  | -                                 |                                        |
| OPC     | 41.6             | 3.66           | 182.3       | 177.1            | 21.9                              | 21.5                                   | 50.6             | 4.27           | 172.9       | 182.9            | 25.9                              | 26.1                                   |
|         |                  | 3.24           | 173.2       |                  | 20.5                              |                                        |                  | 4.33           | 175.1       |                  | 26.8                              |                                        |
|         |                  | 3.55           | 175.7       |                  | 22.0                              |                                        |                  | 4.29           | 200.8       |                  | 25.7                              |                                        |



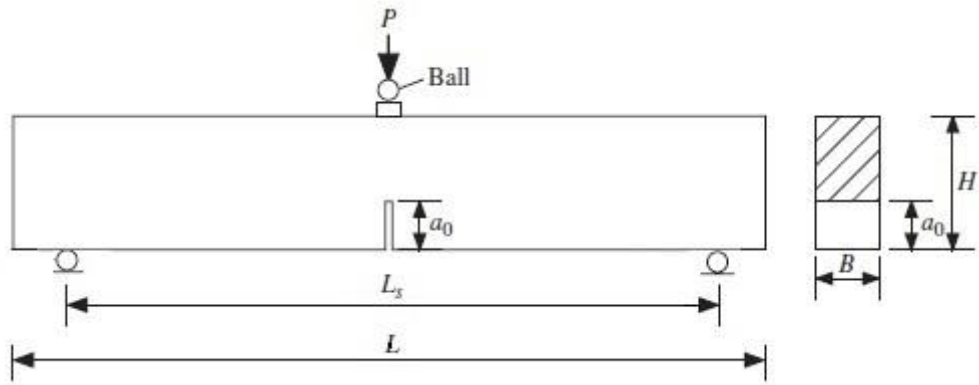


**Fig. 1** Schematic diagram of three-point bending test

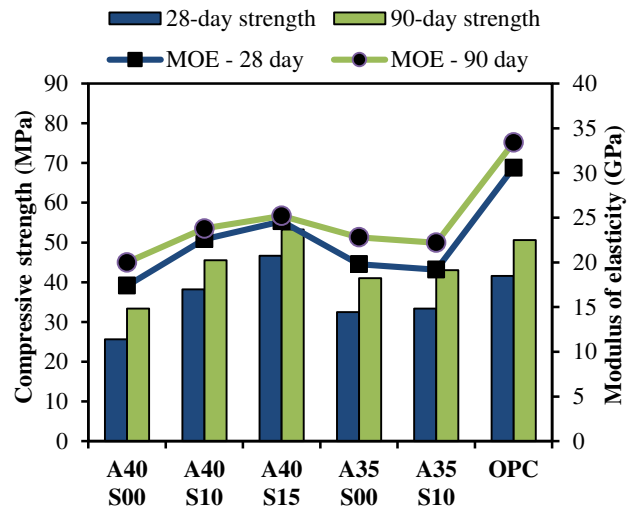
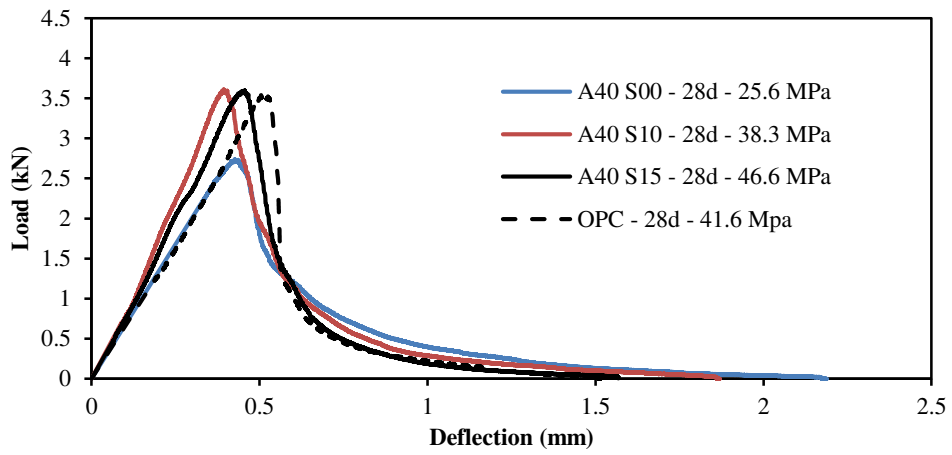
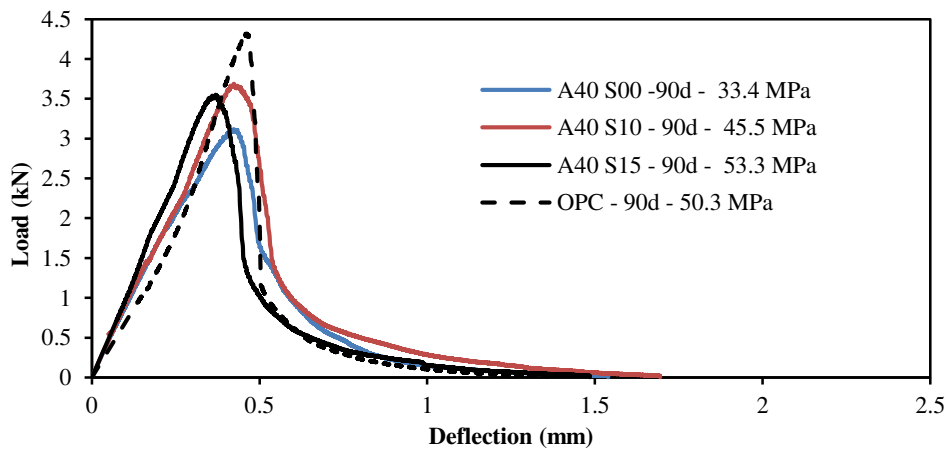


**Fig. 2** Compressive strength and modulus of elasticity of geopolymer and OPC concretes



(a)



(b)

**Fig. 3** Comparison of the load deflection diagrams of geopolymer concretes and OPC concrete at (a) 28 days and (b) 90 days

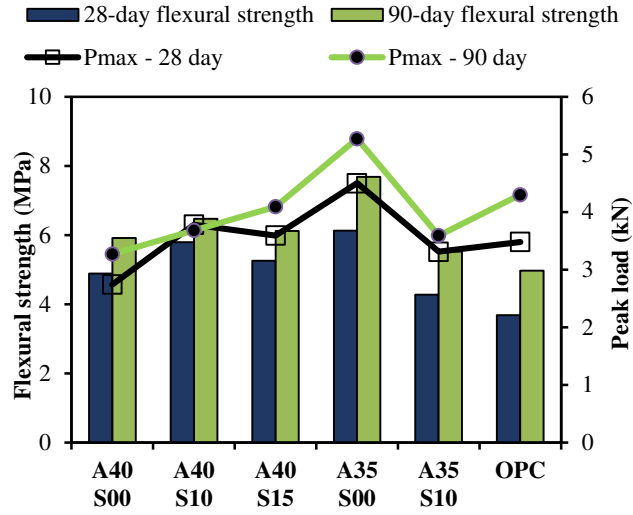


**Fig. 4** Relationship of peak load to flexural strength at 28 day and 90 days

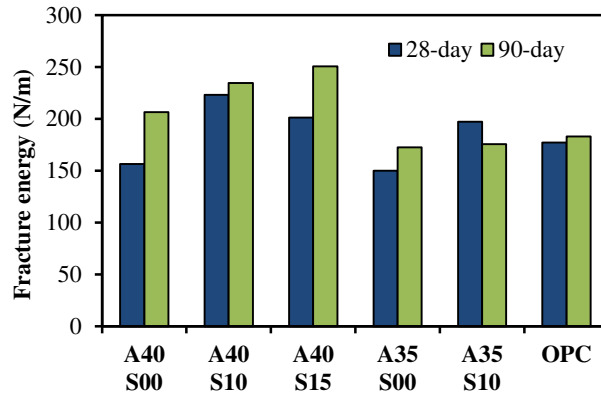


**Fig. 5** Fracture energy of geopolymer and OPC concrete at 28 and 90 days

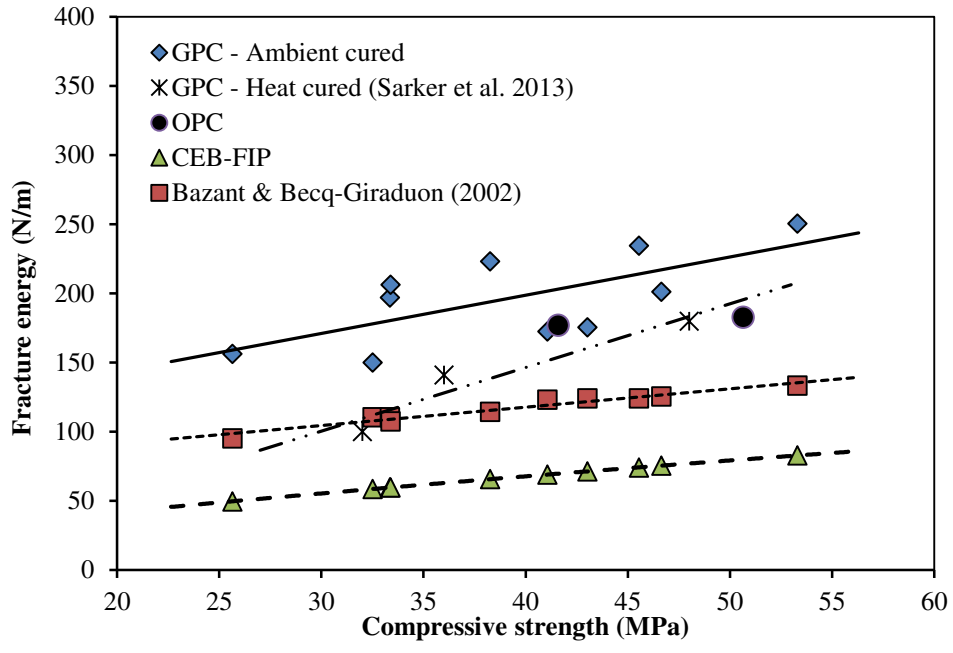


**Fig. 6** Relationship of fracture energy and compressive strength

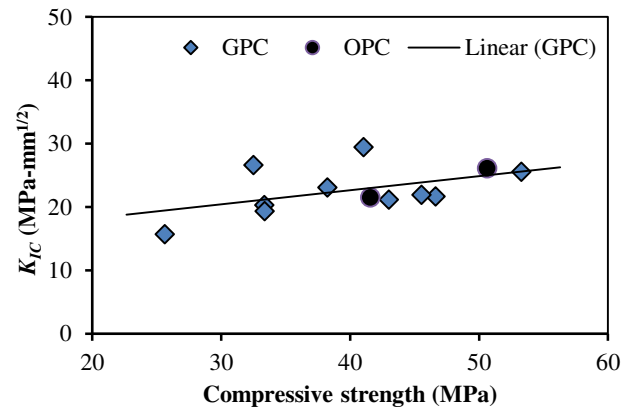


**Fig. 7** Relationship of critical stress intensity factor with compressive strength

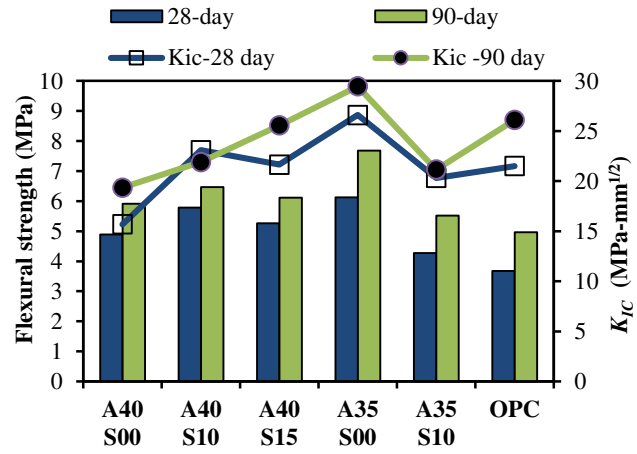


**Fig. 8** Relationship of critical stress intensity factor with flexural strength.